Original Article

Optimal positions of clear aligner attachments to achieve lower canine tipping and bodily movement using finite element analysis

Pin-Yu Chen [a], Heng-Li Huang [a,b,c], Jian-Hong Yu [a,d*], Jui-Ting Hsu [a,b**]

[a] *School of Dentistry, China Medical University, Taichung, Taiwan*
[b] *Department of Biomedical Engineering, China Medical University, Taichung, Taiwan*
[c] *Department of Bioinformatics and Medical Engineering, Asia University, Taichung, Taiwan*
[d] *Department of Dentistry, China Medical University Hospital, Taichung, Taiwan*

Abstract *Background/purpose:* Clear aligners are popular orthodontic tools because of their relatively aesthetic appearance and convenience of use. Nevertheless, bodily tooth movements still present challenges. This study evaluated various configurations of attachments placed on the mandibular canine in terms of the efficiency of canine bodily movement and correction of tipping.

Materials and methods: A finite element model of the mandible was constructed to investigate the effects of various attachment configurations on the overall bodily movement and undesirable tipping of a mandibular canine. Canine movements were categorized into four types, namely tipping and bodily movements in the mesial and distal directions. The size and shape of the attachments were fixed, but their placement and orientation were varied. Five and seven attachment configurations were evaluated for their influence on tipping and bodily movements, respectively.

Results: Attachment configuration significantly influenced mandibular canine tipping. The mesial occlusal—distal cervical and mesial occlusal—mesial cervical configurations had notable effects on mesial tipping, and the mesial occlusal—mesial cervical configuration excelled in distal tipping by increasing strain by 33.1%. The mesial occlusal—mesial cervical attachment configuration consistently had superior efficiency in facilitating both mesial and distal bodily movements of the canine.

* Corresponding author. School of Dentistry, China Medical University, 91 Hsueh-Shih Road, Taichung 40402, Taiwan.
** Corresponding author. Department of Biomedical Engineering, China Medical University, 91 Hsueh-Shih Road, Taichung 40402, Taiwan.
E-mail addresses: kenkoyu@mail.cmu.edu.tw (J.-H. Yu), jthsu@mail.cmu.edu.tw (J.-T. Hsu).

Conclusion: The mesial occlusal—mesial cervical attachment configuration excelled in all four types of canine movement. Irrespective of the attachment configuration, canines tend to move overall with slight tipping due to skeletal resistance and their center of rotation. The attachment configuration is crucial to the success of clear aligner treatment and must be carefully considered in clinical practice.

Introduction

Malocclusion, a prevalent dental condition, encompasses various degrees of dental and skeletal problems with various manifestations, such as crowding, protrusion, and crossbite. Orthodontic treatments, such as traditional fixed orthodontics and clear aligner treatment, aim to correct tooth misalignment, thus improving mastication, oral hygiene, periodontal health, and facial aesthetics and preventing caries. Clear aligner treatment, a modality developed using computer-aided design and engineering, involves the use of transparent plastic trays molded to fit over the teeth. These trays are worn for a specified duration and replaced at regular intervals, and they result in effective alignment of the teeth.

Orthodontic treatment induces teeth movement by applying forces to the teeth, which affect periodontal ligaments (PDLs) and the alveolar bone.[1–3] Traditional stainless steel arch wires may exert excessive force, causing discomfort and slow bone absorption.[4] By contrast, clear aligners, which are made of polymer materials, continuously deliver smaller forces to induce tooth movement. These forces are generated from mismatches between the teeth and the aligners. The teeth gradually move into position as the aligners deform. Patients are required to wear clear aligners for over 22 h every day.

Clear aligners have become increasingly popular because they have several advantages, such as a transparent appearance and easy maintenance. However, they must be frequently changed and are limited in their ability to trigger certain tooth movements. With clear aligners, controlling the torque, root angle adjustments, intrusion, and rotation of teeth, especially rounded teeth such as canines and premolars, is difficult. These difficulties lead to inaccurate movements due to insufficient interproximal undercuts, resulting in an uneven force distribution.[5–7] Poor retention and inadequate adaptation exacerbate these issues. Orthodontists may not recommend choosing clear aligner in cases where tooth extraction is required to achieve bodily tooth movement because the use of clear aligners entails the application of complex forces.[8,9] To address this problem of restricted tooth movement, orthodontists and dental engineers design attachments that contribute to force application and aligner retention.[10] Treatment accuracy is affected by factors such as aligner material, thickness, attachment design, and tooth morphology.

This paper presents a finite element model of the dental system, encompassing the mandibular tooth with its surrounding structures and clear aligners with their attachments. To explore the influence of various clear aligner attachments, we utilized finite element analysis software to simulate two quarter-ellipsoid attachments or a single rectangular attachment at different positions and orientations on the buccal side of the mandibular canine and compared the biomechanical responses and tooth movement effects elicited by the different attachments. The results of this study give orthodontists insights into how clear aligners can be effectively designed to enhance treatment outcomes.

Materials and methods

Mandible finite element model construction

The study protocol was approved by the Institutional Review Board of China Medical University Hospital (approval no. CMUH112-REC1-095). A comprehensive finite element model of the mandible was created based on a digital model derived from a cone-beam computed tomography (CBCT) scan obtained from China Medical University Hospital in Taichung, Taiwan, with the patient's CBCT data post-processed using Mimics software (Materialise, Leuven, Belgium) (Fig. 1). We modeled cortical bone, cancellous bone, gingiva, and the PDLs with a thickness of 0.25 mm, with the model covering the central incisor to the first molar. To simplify the model, we modeled only the left side of the mandible. The target tooth for our analysis was the mandibular canine. We excised the bony segment of interest, spanning from the mesial side of the central incisor to the distal side of the first molar. This sample enabled us to examine the region of interest in high detail.

After the finite element model of the mandibular bone was constructed, quarter-ellipsoid (2.0 mm × 2.0 mm × 1.0 mm) and rectangular (2.0 mm × 3.0 mm × 1.0 mm) attachments were designed. The size and shape of the attachments were fixed, but their placement and orientation on the buccal side of the mandibular canine were varied. Subsequently, corresponding clear aligners with an average thickness of 0.5 mm were modeled. The quarter-ellipsoid attachments were modeled in pairs in different orientations and positions on the mandibular canine. The buccal surface was divided into nine sections, and the attachments were positioned at the intersections. The rectangular attachment was positioned at the center of the buccal side of the canine.
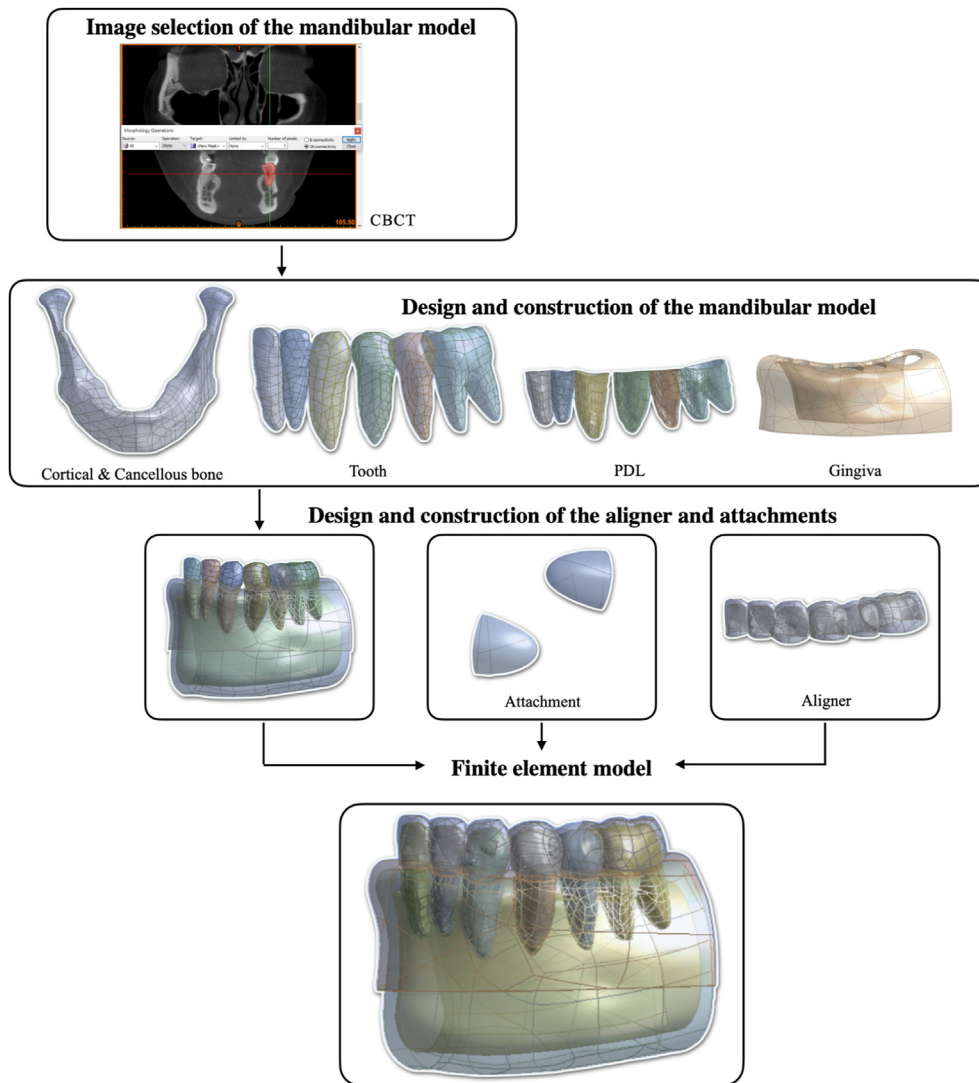
Figure 1 Assembly of the finite element model.

Canine tooth movements were categorized into four groups (Fig. 2): Group 1, mesial tipping with five configurations; Group 2, distal tipping with five configurations; Group 3, mesial bodily movement with seven configurations, and Group 4, distal bodily movement with seven configurations.

A total of 24 attachment designs were evaluated. Each attachment design was named after the canine movement direction associated with it and the position on the buccal side of the canine where it was placed. For example, in the mesial tipping group, the first design involved placing attachments separately on the mesial cervical and distal occlusal surfaces. The rectangular attachment served as the control, and results were compared against it to assess variation among the groups.

The assembled model components were imported into the ANSYS Workbench (Swanson Analysis, Canonsburg, PA, USA) for meshing. A four-node tetrahedral element was constructed, and material properties were assigned to the respective regions.

Material properties and contact interaction

Except for the PDL of the target mandibular canine, which was assigned a "multilinear isotropic hardening" property, all components were defined as "isotropic elastic" materials (Table 1). The "multilinear isotropic hardening" property indicated that the material's behavior could be divided into two distinct stages. Specifically, after the PDL of the canine experienced a certain level of force, its material property transitioned from an initial modulus E_1 to a new modulus E_2. Initially, the PDL exhibited a Young's elastic modulus E_1 of 0.15 MPa. Upon the reaching of strain $E_{12} = 6.3\%$, the PDL characteristic underwent a transition, and its Young's elastic modulus E_2 became 0.6 MPa. Thus, beyond a specific force level, the PDL significantly stiffened. The parameters were based on the results of Kawarizadeh et al.[11]

The interfacial surfaces between the clear aligner and the teeth and attachments were designated as contact surfaces. On the basis of the literature, the frictional co-efficient was set to 0.2. Bonded contacts were assumed
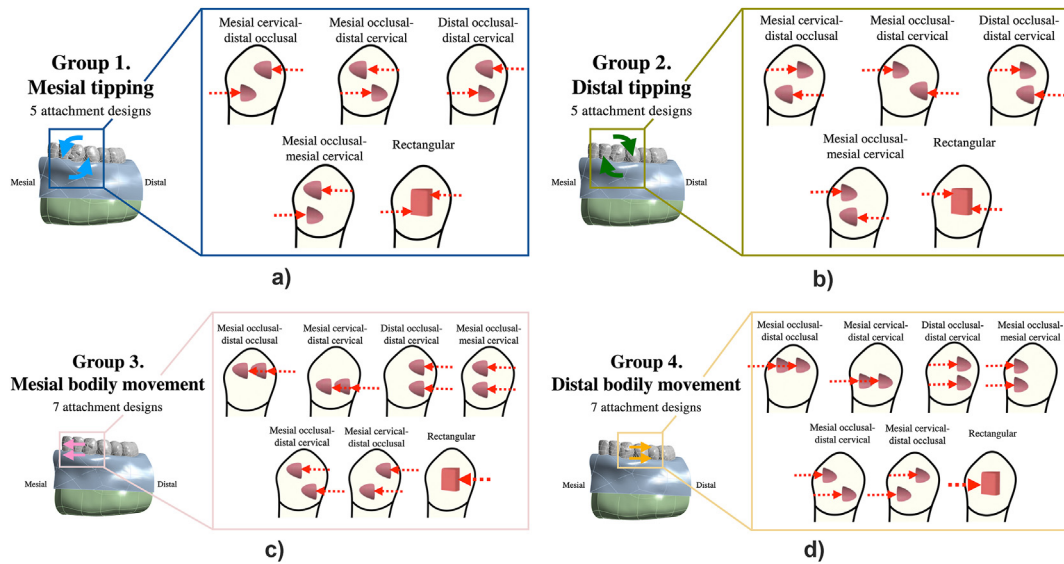
Figure 2 Various attachment designs for the four types of canine movement: (a) mesial and (b) distal tipping movement, and (c) mesial and (d) distal bodily movement; A pair of 5.91-N forces were applied perpendicularly to the cut surface of each quarter-ellipsoid attachment and the mesial and distal aspect of the rectangular attachment (shown in red dashed arrow).

Table 1 Material properties of the components of the finite element model.

Components	Elastic modulus (MPa)	Poisson's ratio	Reference
Cortical bone	14,900	0.3	12,13,14
Cancellous bone	460	0.3	
Gingiva	2.8	0.4	15
PDL linear	0.71	0.4	16
Bilinear PDL for canine	$E_1 = 0.15$; $E_2 = 0.6$; Ultimate strain $E_{12} = 6.3\%$	0.3	11
Tooth	18,600	0.3	13,14,17
Attachment	12,500	0.36	18
Aligner (Thermoplastic polyurethane)	1900	0.49	19

between the cortical and cancellous bones, the cortical bone and the gingiva, the PDL and the corresponding alveolar bone and tooth surfaces, and the tooth and attachment surfaces.[9,15,20]

Loading and boundary conditions

The loading conditions were based on the approach adopted by Kim et al.[21] A force of 5.91 N was applied to the cut surfaces of each quarter-ellipsoid attachment (Fig. 2 shown in red dashed arrow). This setup was derived from a study reporting that achieving a tooth movement of 0.5 mm requires a force of approximately 11.82 N.[22] Considering that a single clear aligner typically induces tooth movements of 0.2—0.4 mm, a reduced force of 5.91 N (half of 11.82 N) was applied in this study to simulate an anticipated displacement of approximately 0.25 mm. This force represents the orthodontic load generated by the clear aligner when it is pressed against the attachments during intraoral wear. Regarding the boundary conditions, we fixed to zero the degrees of freedom along the X, Y, and Z axes for the cut edges of the bone and gingival segments on both sides (Fig. 3).

Based on the material properties, loading conditions, and boundary conditions established in the preceding sections, we performed a series of convergence analyses of the PDL model. The effects of the mesh size and element counts were investigated. The convergence criterion employed in this study was an error limit of 4% in the measurement of the von Mises strain within the PDL.
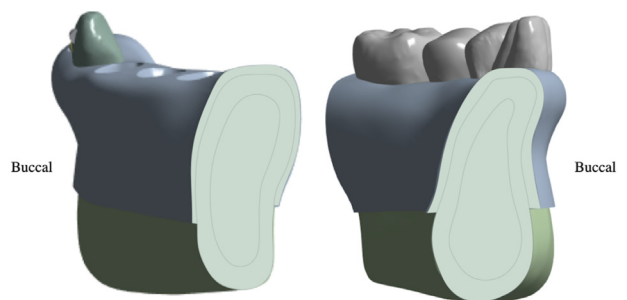

Figure 3 Boundary conditions were fixed at the cut edges of the bone and gingival segments on both sides (shown in light green).

Convergence test and evaluation indices

Five mesh sizes were evaluated in the model convergence analysis to determine the configuration that achieved convergence. The results indicated that convergence was achieved with element sizes of 1.0 mm for the cortical bone, cancellous bone, and gingiva; 0.47 mm for the teeth; 0.3 mm for the attachments; 0.25 mm for the clear aligner; and 0.2 mm for the PDL. This mesh size combination was adopted as the standard for subsequent analyses.

The von Mises strain that develops within the PDL serves as an indicator of PDL deformation and is considered a key factor in bone remodeling.[23,24] Therefore, in accordance with the literature, PDL strain was employed as the metric for evaluating the efficacy of canine tooth movement. Furthermore, cortical bone and cancellous bone are intricately interconnected structures within human tissues. The mild and continuous orthodontic forces exerted by clear aligners on specific tooth surfaces are transmitted to the adjoining osseous tissues, where they induce bony changes and enable movement of teeth toward the desired positions. Frost's mechanostat highlights the diverse range of responses that bone can exhibit depending on different strain level thresholds. Consequently, our study considered the von Mises strain that developed within the alveolar bone surrounding the mandibular canine as a key indicator of the bone remodeling induced by the clear aligner.[25,26]

Results

The various attachment designs resulted in diverse biomechanical reactions and force systems in the simulations of bodily tooth movement and tipping of the mandibular canine. The following sections present the results obtained regarding strain development within the PDL and surrounding bone tissue.

Von Mises strain results for the PDL

When mesial tipping of the canine was simulated, the distribution of the maximum strain along the root height was inconsistent. The strain was biased toward the distal buccal side for all attachment configurations except mesial cervical−distal occlusal. The von Mises strains were similar for the mesial cervical−distal occlusal (0.0350) and distal occlusal−distal cervical (0.0355), mesial occlusal−distal cervical (0.0470) and mesial occlusal−mesial cervical (0.0469) configurations (Fig. 4).

Regarding distal tipping of the canine, the von Mises strain distribution on the PDL was located near the root apex for all attachment configurations except mesial cervical−distal occlusal and the rectangular attachment. Notably, the maximum strain associated with the mesial occlusal−mesial cervical configuration (0.0426) was 1.9 times that associated with the mesial occlusal−distal cervical configuration (0.0223; Fig. 5).

Regarding mesial bodily movement of the canine, the maximum von Mises strain distribution was mainly concentrated near the cervical region of the buccal side of the PDL. For distal bodily movement of the canine, the maximum von Mises strain distribution was also centered at the cervical region, but it covered the area from the mesial buccal to the mesial lingual side. For both these canine movements, the mesial occlusal−mesial cervical configuration generated the maximum von Mises strains (0.2397 and 0.2876, respectively). Additionally, the strains produced by the two bodily movements of the canine were 5−10 times higher than those produced by the two tipping movements of the canine (Figs. 6 and 7).

Von Mises strain results for the surrounding bone

The maximum von Mises strains (and corresponding attachment configurations) generated in the cancellous bone surrounding the mandibular canine during different
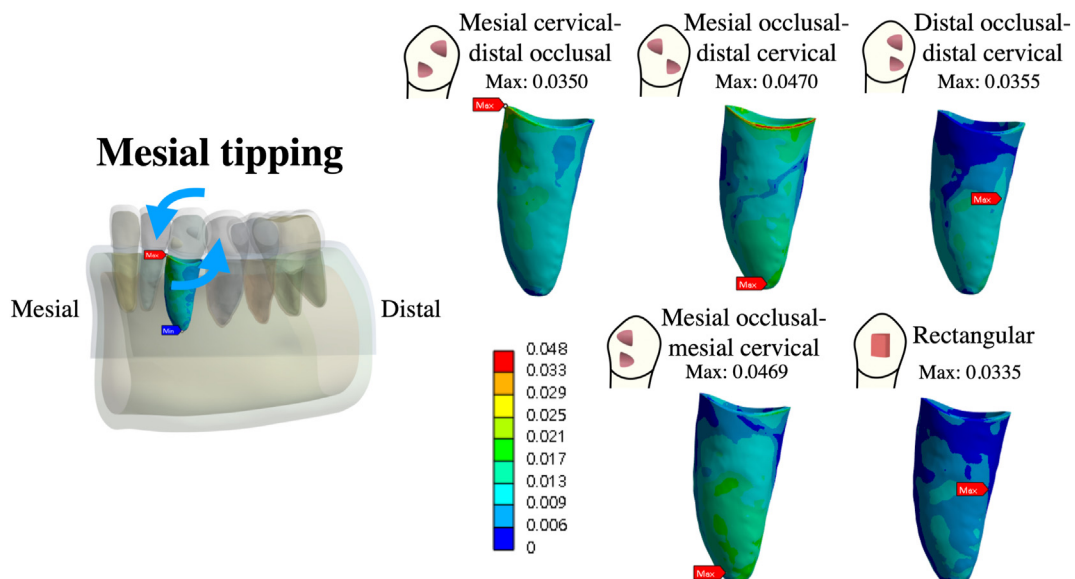

Figure 4 Von Mises strain in the PDL of the mandibular canine for mesial tipping movement.
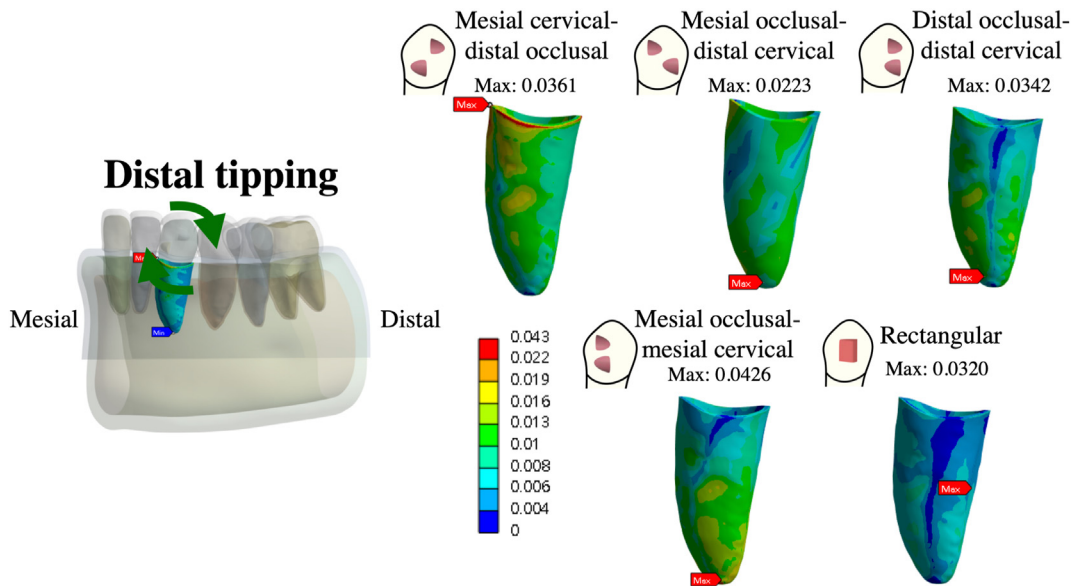
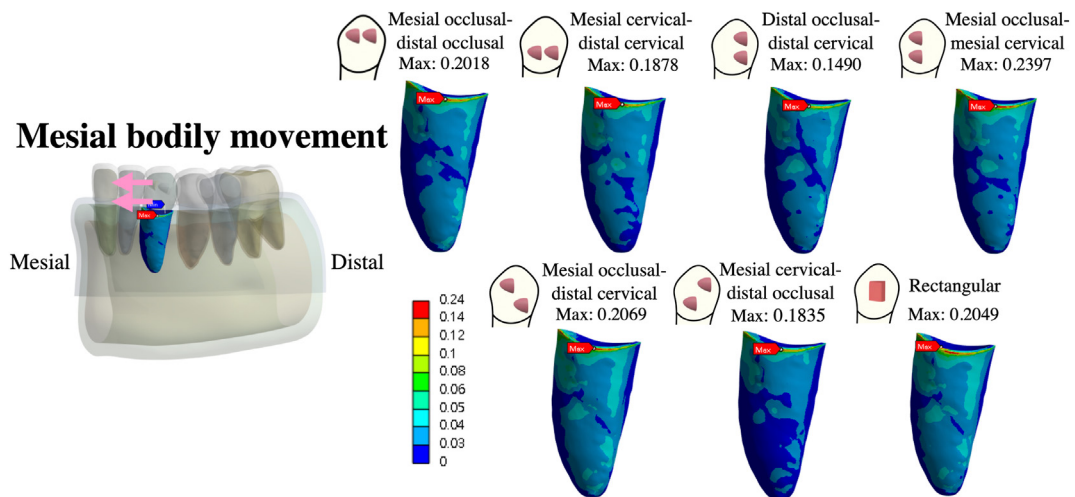**Figure 5** Von Mises strain in the PDL of the mandibular canine for distal tipping movement.

Figure 6 Von Mises strain in the PDL of the mandibular canine for mesial bodily movement.
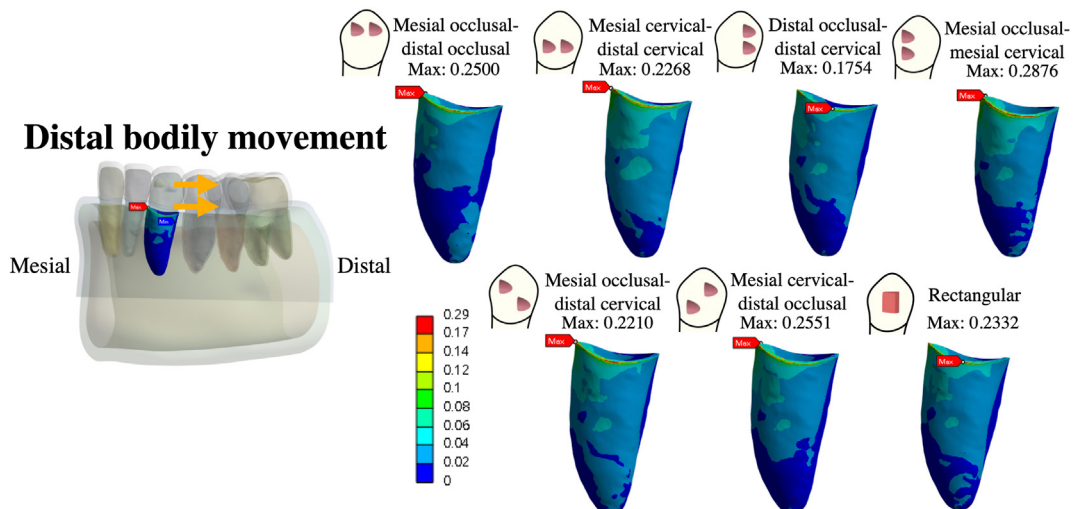

Figure 7 Von Mises strain in the PDL of the mandibular canine for distal bodily movement.

canine movements were as follows: mesial tipping movement, mesial cervical–distal occlusal configuration (36.405 μ); distal tipping movement, mesial cervical–distal occlusal configuration (44.32 μ); mesial bodily movement, rectangular configuration (186.64 μ); and distal bodily movement, mesial occlusal–mesial cervical configuration (137.04 μ; Fig. 8 and Table 2).

The maximum von Mises strains (and corresponding attachment configurations) generated in the cortical bone surrounding the mandibular canine during different canine movements were as follows: mesial tipping movement, mesial occlusal–distal cervical configuration (42.688 μ); distal tipping movement, mesial cervical–distal occlusal configuration (40.956 μ); mesial bodily movement, mesial occlusal–mesial cervical configuration (232.25 μ); and distal bodily movement, mesial occlusal–mesial cervical configuration (212.97 μ). On average, the two bodily movements of the canine generated strains that were 5–10 times higher than those generated in the two tipping movements of the canine (Fig. 9 and Table 2).

Discussion

This study aimed to enhance the bodily movement efficiency of canines and their correct tipping during clear aligner treatment, which can ensure congruent movement of the crown and the root. Unlike prior research—which has explored factors such as aligner thickness, material properties, and auxiliary components—this study uniquely utilized finite element analysis involving bilinear material characterization of the PDL. The performance of different configurations of quarter-ellipsoid attachment pairs was compared between configurations and with the performance of a traditional rectangular attachment. Vertically oriented attachment pairs positioned on the mesial aspect of the canine's buccal surface were discovered to have the

highest efficacy. Such attachments were found to effectively induce the physiological responses necessary for tooth movement because they transmitted the appropriate forces and elicited biomechanical responses. These findings will inform the design of attachments that enable more precise control of tooth movement, thereby improving the treatment outcomes of clear aligner therapy.

In 2015, Gomez et al.[9] constructed a three-dimensional finite element dental model to simulate the effects of clear aligner attachments on the bodily movement of maxillary canines. Their results revealed that use of the attachments was associated with controlled bodily movement of the teeth, whereas nonuse of the attachments resulted in undesirable uncontrolled tipping. In 2019, Goto et al.[27] used finite element analysis to show that attachment shape and placement location did not strongly influence the translational forces generated and the tipping moments in the horizontal or vertical direction. On the basis of these findings, we chose the commonly used quarter-ellipsoid and rectangular attachments for this investigation in this study. We fixed these shapes and also the height of the attachments on the buccal side of the mandibular canines; the only parameters that were varied were the placement location and orientation of the attachments.

We discovered that for mesial canine tipping, the mesial occlusal–distal cervical and mesial occlusal–mesial cervical attachment configurations produced the highest von Mises strain values, which suggested that the strain distributions associated with these two configurations were similar. Conversely, the rectangular attachment produced the smallest strain. During distal tipping of the canine, the mesial occlusal–mesial cervical configuration induced the highest von Mises strain, whereas the mesial occlusal–distal cervical configuration induced a strain that was even smaller than that induced by the control attachment, implying less favorable distal tipping movement. For
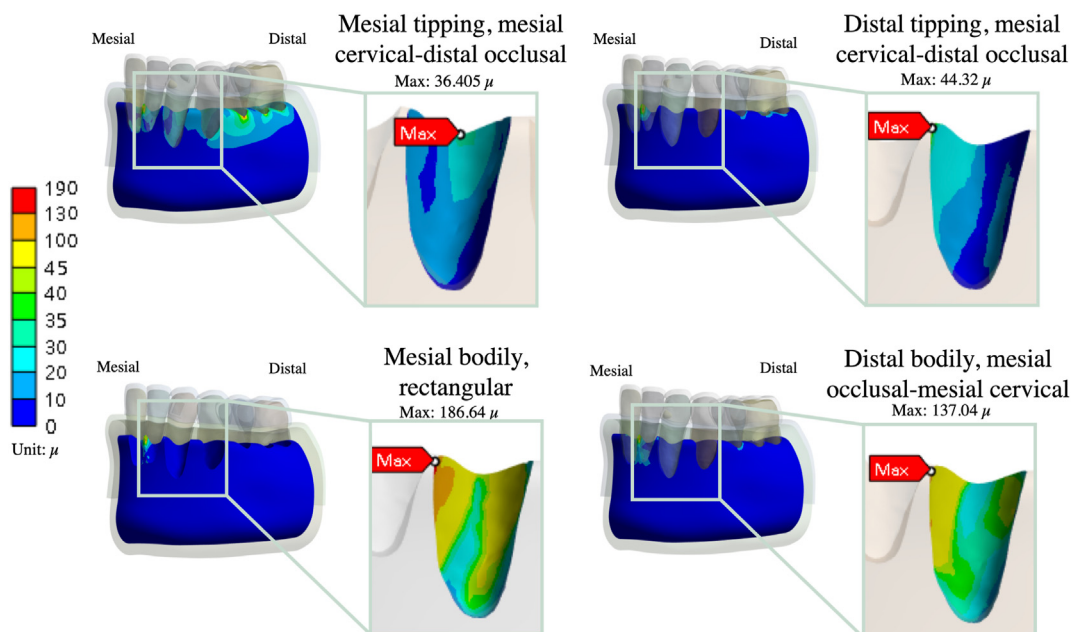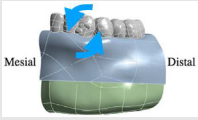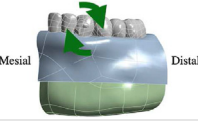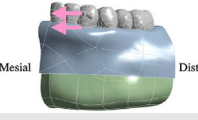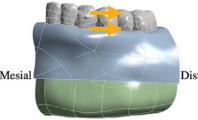

Figure 8 Maximum result values of von Mises strain in cancellous bone.

Table 2 Von Mises strain values in cortical bone and cancellous bone during (a) mesial tipping movement, (b) distal tipping movement, (c) mesial bodily movement, and (d) distal bodily movement.

vM strain (μ)	Mesial cervical-distal occlusal	Mesial occlusal-distal cervical	Distal occlusal-distal cervical	Mesial occlusal-mesial cervical	Rectangular
(a) Mesial tipping movement					
cancellous	36.405	27.129	23.427	27.307	24.354
cortical	30.626	42.668	11.421	13.681	11.503
(b) Distal tipping movement					
cancellous	44.32	19.431	42.223	36.103	33.462
cortical	40.956	30.223	12.41	8.229	10.286

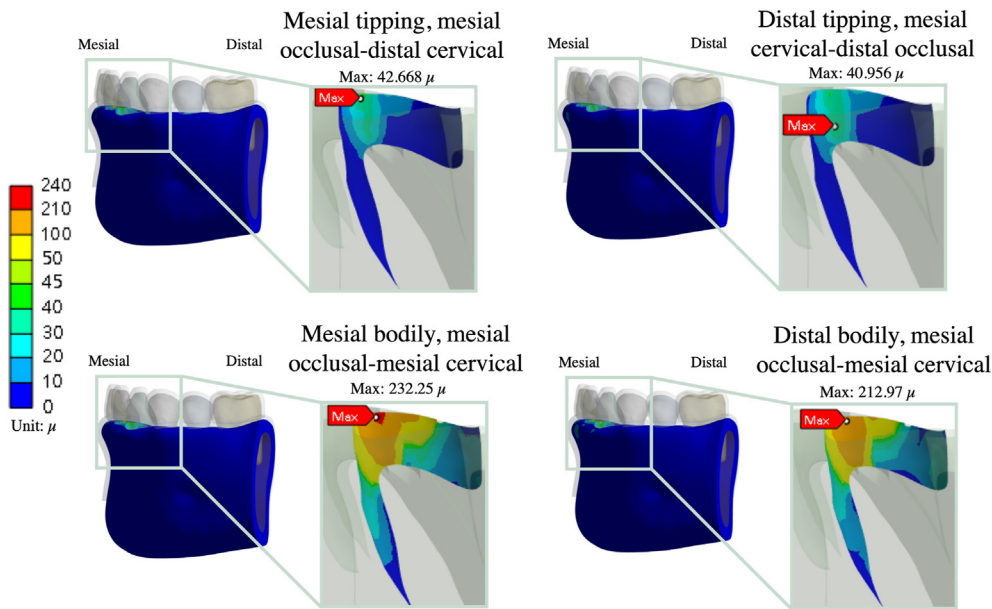| vM strain (μ)	Mesial occlusal-distal occlusal	Mesial cervical-distal cervical	Distal occlusal-distal cervical	Mesial occlusal-mesial cervical	Mesial occlusal-distal cervical	Mesial cervical-distal occlusal	Rectangular
(c) Mesial bodily movement							
cancellous	161.56	181.94	162.04	184.03	176.84	168.07	186.64
cortical	197.13	190.05	156.38	232.25	199.34	188.71	202.85
(d) Distal bodily movement							
cancellous	107.79	125.42	98.17	137.04	120.29	113.44	130.42
cortical	168.91	163.06	121.78	212.97	171.37	160.84	180.17

Figure 9 Maximum result values of von Mises strain in cortical bone.

both mesial and distal bodily movements of the canine, vertically oriented attachment pairs positioned on the mesial aspect (mesial occlusal—mesial cervical) demonstrated superior efficacy, highlighting their potential to enhance the canine movement efficiency. Conversely, vertically oriented attachment pairs placed on the distal aspect (distal occlusal—distal cervical) yielded poorer results than rectangular attachments, indicating lower efficiency.

In this study, the maximum strains were predominantly distributed along the cervical area of the PDL for bodily movement in the mesial and distal directions. This distribution suggests that the orthodontic forces primarily acted on the clinical crown rather than being uniformly distributed across the center of the tooth, resulting in slight tipping rather than bodily movement of the canine, as simulated in our study. In addition, the cervix of the tooth, where the PDL interfaces with the alveolar bone, is crucial in the biomechanical behavior of teeth, especially under orthodontic forces. This is because the tooth primarily contacts the alveolar bone in this area, making it a focal point for force transmission. In addition to the location of force transmission, the strain distribution is directly influenced by the accuracy of the model setup, discontinuities in the geometric shapes of components, and the specified boundary conditions. Therefore, more precise model configuration can better simulate the anatomical structure and material properties of the PDL, which are critical factors for understanding and simulating tooth responses during orthodontic treatment. In 2021, Ho et al.[28] fabricated resin typodont models by using a three-dimensional printer and designed three attachment shapes (thick and thin ellipsoid and rectangular attachments) in combination with three clear aligner materials to analyze the bodily movement of canines. Their study found that none of the three attachment designs induced true bodily movement of the teeth but instead caused tipping movements, which

corroborates our findings. This suggests that the forces transmitted by attachments may not adequately facilitate the bodily movement of canines.

Frost's mechanostat theory offers a framework for understanding how bone responds biologically to changes in loads. It emphasizes the diverse responses that bone may exhibit at different strain thresholds, including disuse atrophy, an adapted state, physiological overload, pathological overload, and fracture. Ideally, bone strain should remain within the adapted state threshold (1000—1500 μ) to optimize bone strength and maintain stability by resisting and repairing microdamage.[25,26] In this study, the maximum strain in the bone surrounding the mandibular canine did not exceed the adapted state threshold designated by Frost's mechanostat theory (1000 μ); these small strains could thus lead to bone remodeling and decrement of the bone density in response to the dynamic situation between masticatory loading and orthodontic forces.

Under the biomechanical stress produced by orthodontic appliances, orthodontic tooth movement is dependent upon alveolar bone remodeling, which includes osteoblasts' production and deposition of bone on the tension side and osteoclasts' resorption of bone on the pressure side.[29] Studies have revealed that alveolar bone density decreased after orthodontic treatment of rat teeth,[30,31] likely due to force-induced bone absorption and generation, resulting in initially lower-density woven bone that was not completely mineralized.[32,33] Additionally, Hsu et al. reported an approximately 24% decrease in bone density around the maxillary central incisors, lateral incisors, and canines after orthodontic treatment, as measured using CBCT.[34,35] Furthermore, the decrease in alveolar bone density was greater on the compression side of tooth movement. Scholars believe that our result should be attributed to finite element modeling simulating the initial state of teeth under force. Although bone formation should occur on the tension side, the density remains

relatively low due to newly formed bone, which must undergo continuous bone remodeling in the future if it is to acquire the original bone's density. Doctors suggested wearing orthodontic retainers for a period of time while the low-density woven bone mineralizes into strong lamellar bone following active orthodontic treatment to straighten the alignment of the tooth.[36]

In contrast to past studies, this study advocates for the utilization of repeatable and noninvasive finite element analysis to construct digital dental models for simulating clear aligner treatment. We investigated the effects of different clear aligner attachments on treatment efficacy and compared various attachment configurations to determine the optimum configuration for enhancing the overall bodily movement of canines and mitigating undesirable tipping. Many studies have indicated that clear aligner treatment with the precise use of attachments achieves better movement efficiency than does treatment without attachments. We selected the commonly used quarter-ellipsoid and rectangular attachments, which were of fixed size and shape, and explored the influences of their placement and orientation on treatment efficacy. We comprehensively discussed how these factors can potentially affect treatment outcomes, addressing topics that were left unaddressed in previous studies.

Simulations can accurately replicate effects under various conditions when parameters such as material properties of attachments and aligners, as well as loading and boundary conditions, are adjusted to provide comprehensive and diverse reference data. For instance, various attachment materials, designs, or aligner materials can be studied to optimize treatment outcomes. Given the unique geometrical structures of the maxilla, the mandible, and individual teeth, generalizing these findings to other teeth beyond the mandibular canines may be challenging. Therefore, exploring the responses of all teeth is essential. Additionally, the model assumed that the cortical bone was a homogeneous 2.0-mm-thick layer with isotropic material properties; thus, the model did not reflect the heterogeneous nature of the human jaw bone. Although this assumption aided model tractability, it must be acknowledged as a limitation. Furthermore, factors such as mesh refinement and loading conditions, which simulated a pair of 5.91-N orthodontic force vectors, may have affected the model's performance and clinical extrapolation.

This study utilized a finite element model to analyze biomechanical responses within the PDL of the mandibular canines. Compared with *in vitro* mechanical experiments, finite element simulations can be used to quickly and repetitively evaluate the performance of multiple treatment schemes and thus can reduce the experimental cost and time. These simulations effectively illustrate complex and microscopic biomechanical responses during orthodontic treatment, such as stress distribution, aligner deformation, and tooth movement. Understanding these responses is crucial for elucidating the mechanisms underlying the function of clear aligners. Similar to prior research, our study did not conduct *in vitro* experiments to validate the model.[9,18,21] However, reference to previous studies instils confidence in our simulation results, particularly those regarding observed trends. Future efforts should prioritize *in vitro* experimental validation to bolster

the reliability of our findings. Additionally, exploring the effects of different parameters on clear aligner treatment and incorporating complex intraoral force dynamics would likely facilitate the identification of the most effective and suitable treatment methods for individual patients.

This study investigated four types of canine movement, namely tipping and bodily movements in the mesial and distal directions. The objective was to determine the optimal shape and position of attachments for improving the efficiency of canine bodily movement during clear aligner therapy. For mesial tipping of the canine, the mesial occlusal—mesial cervical and mesial occlusal—distal cervical attachment configurations produced similar strains in the PDL and were found to have key roles in guiding this canine movement. For distal tipping of the canine, the mesial occlusal—mesial cervical attachment configuration produced the highest strain, 33.1% higher than the baseline; the configuration thus favorably facilitates this canine movement. For both mesial and distal bodily movements of the canine, the mesial occlusal—mesial cervical attachment configuration produced the highest strain and thus had excellent efficiency in promoting overall canine movement. In clear aligner treatment, the choice of appropriate auxiliary tools (clear aligner attachments, intermaxillary elastics, orthodontic mini-implants, etc.) can significantly influence the effectiveness of the treatment. These choices not only affect patient comfort but also directly influence the speed and outcome of orthodontic treatment.

Declaration of competing interest

The authors have no conflicts of interest relevant to this article.

Acknowledgment

References

1. Bergomi M, Wiskott HA, Botsis J, Mellal A, Belser UC. Load response of periodontal ligament: assessment of fluid flow, compressibility, and effect of pore pressure. *J Biomech Eng* 2010;132:e014504.
2. Natali AN, Carniel EL, Pavan PG, Sander FG, Dorow C, Geiger M. A visco-hyperelastic-damage constitutive model for the analysis of the biomechanical response of the periodontal ligament. *J Biomech Eng* 2008;130:e031004.
3. Proffit WR, Fields HW, Larson BE, Sarver DM. *Contemporary orthodontics*, 6th ed. Philadelphia: Elsevier, 2019.
4. Bae GS. Clinical limitations and its solutions of the clear overlay appliance treatment. *J Korean Dent Assoc* 2016;54: 563—74.
5. Rossini G, Parrini S, Castroflorio T, Deregibus A, Debernardi CL. Efficacy of clear aligners in controlling orthodontic tooth movement: a systematic review. *Angle Orthod* 2015;85:881—9.
6. Bowman SJ. Improving the predictability of clear aligners. *Semin Orthod* 2017;23:65—75.
7. Lu TY, Ahmad MA, Hassan WNW, Hariri F. The stress and deformation effect of novel rapid maxillary expanders by finite element analysis. *J Med Biol Eng* 2022;42:397—403.

8. Karras T, Singh M, Karkazis E, Liu D, Nimeri G, Ahuja B. Efficacy of invisalign attachments: a retrospective study. *Am J Orthod Dentofacial Orthop* 2021;160:250—8.

9. Gomez JP, Pena FM, Martinez V, Giraldo DC, Cardona CI. Initial force systems during bodily tooth movement with plastic aligners and composite attachments: a three-dimensional finite element analysis. *Angle Orthod* 2015;85:454—60.

10. Nucera R, Dolci C, Poetelli M, et al. Effects of composite attachments on orthodontic clear aligners therapy: a systematic review. *Materials* 2022;15:e533.

11. Kawarizadeh A, Bourauel C, Jäger A. Experimental and numerical determination of initial tooth mobility and material properties of the periodontal ligament in rat molar specimens. *Eur J Orthod* 2003;25:569—78.

12. Poppe M, Bourauel C, Jäger A. Determination of the elasticity parameters of the human periodontal ligament and the location of the center of resistance of single-rooted teeth a study of autopsy specimens and their conversion into finite element models. *J Orofac Orthop* 2002;63:358—70.

13. Huang HL, Tsai MT, Yang SG, Su KC, Shen YW, Hsu JT. Mandible integrity and material properties of the periodontal ligament during orthodontic tooth movement: a finite-element study. *Appl Sci* 2020;10:e2980.

14. Tsai MT, Huang HL, Yang SG, Su KC, Fuh LJ, Hsu JT. Biomechanical analysis of occlusal modes on the periodontal ligament while orthodontic force applied. *Clin Oral Invest* 2021;25:5661—70.

15. Hong K, Kim WH, Eghan-Acquah E, Lee JH, Lee BK, Kim B. Efficient design of a clear aligner attachment to induce bodily tooth movement in orthodontic treatment using finite element analysis. *Materials* 2021;14:e4926.

1.. Caballero GM, Carvalho Filho OA, Hargreaves BO, Brito HH, Magalhaes Junior PA, Oliveira DD. Mandibular canine intrusion with the segmented arch technique: a finite element method study. *Am J Orthod Dentofac Orthop* 2015;147:691—7.

17. Leung MT, Lee TC, Rabie AB, Wong RW. Use of miniscrews and miniplates in orthodontics. *J Oral Maxillofac Surg* 2008;66:1461—6.

18. Cortona A, Rossini G, Parrini S, Deregibus A, Castroflorio T. Clear aligner orthodontic therapy of rotated mandibular round-shaped teeth: a finite element study. *Angle Orthod* 2020;90:247—54.

19. Jindal P, Worcester F, Siena FL, Forbes C, Juneja M, Breedon P. Mechanical behaviour of 3D printed vs thermoformed clear dental aligner materials under non-linear compressive loading using FEM. *J Mech Behav Biomed Mater* 2020;112:e104045.

20. Yokoi Y, Arai A, Kawamura J, Uozumi T, Usui Y, Okafuji N. Effects of attachment of plastic aligner in closing of diastema of maxillary dentition by finite element method. *J Healthc Eng* 2019;2019:1—6.

21. Kim WH, Hong K, Lim D, Lee JH, Jung YJ, Kim B. Optimal position of attachment for removable thermoplastic aligner on the lower canine using finite element analysis. *Materials* 2020;13:e3369.

22. Li X, Ren C, Wang Z, Zhao P, Wang H, Bai Y. Changes in force associated with the amount of aligner activation and lingual bodily movement of the maxillary central incisor. *Korean J Orthod* 2016;46:65—72.

23. McCormack SW, Witzel U, Watson PJ, Fagan MJ, Gröning F. Inclusion of periodontal ligament fibres in mandibular finite element models leads to an increase in alveolar bone strains. *PLoS One* 2017;12:e0188707.

24. Papageorgiou SN, Keilig L, Hasan I, Jäger A, Bourauel C. Effect of material variation on the biomechanical behaviour of orthodontic fixed appliances: a finite element analysis. *Eur J Orthod* 2016;38:300—7.

25. Kan JPM, Judge RB, Palamara JEA. In vitro bone strain analysis of implant following occlusal overload. *Clin Oral Implants Res* 2014;25:73—82.

26. Robling AG, Daly R, Fuchs RK, Burr DB. Mechanical adaptation. Cambridge: MA. In: *Basic and applied bone biology*, 2nd ed. 2019:203—33.

27. Goto M, Yanagisawa W, Kimura H, Inou N, Maki K. A method for evaluation of the effects of attachments in aligner-type orthodontic appliance: three-dimensional finite element analysis. *Orthod Waves* 2019;76:207—14.

28. Ho CT, Huang YT, Chao CW, Huang TH, Kao CT. Effects of different aligner materials and attachments on orthodontic behavior. *J Dent Sci* 2021;16:1001—9.

29. Xi X, Li ZX, Zhao Y, Liu H, Chen S, Liu DX. N-acetylcysteine promotes cyclic mechanical stress-induced osteogenic differentiation of periodontal ligament stem cells by down-regulating Nrf2 expression. *J Dent Sci* 2022;17:750—62.

30. Bridges T, King G, Mohammed A. The effect of age on tooth movement and mineral density in the alveolar tissues of the rat. *Am J Orthod Dentofac Orthop* 1998;93:245—50.

31. Verna C, Zaffe D, Siciliani G. Histomorphometric study of bone reactions during orthodontic tooth movement in rats. *Bone* 1999;24:371—9.

32. Simmons DJ, Chang SL, Russell JE, Grazman B, Webster D. The effect of protracted tetracycline treatment on bone growth and maturation. *Clin Orthop Relat Res* 1983;180:253—9.

33. Russell JE, Grazman B, Simmons DJ. Mineralization in rat metaphyseal bone exhibits a circadian stage dependency. *Proc Soc Exp Biol Med* 1984;176:342—5.

34. Hsu JT, Chang HW, Huang HL, Yu JH, Li YF, Tu MG. Bone density changes around teeth during orthodontic treatment. *Clin Oral Invest* 2011;15:511—9.

35. Chang HW, Huang HL, Yu JH, Hsu JT, Li YF, Wu YF. Effects of orthodontic tooth movement on alveolar bone density. *Clin Oral Invest* 2012;16:679—88.

36. Yu JH, Huang HL, Liu CF, et al. Does orthodontic treatment affect the alveolar bone density? *Medicine (Baltimore)* 2016;95:e3080.